Further Studies of Fluid Flow and Mass Transfer in Trickle Beds

W. E. SCHIESSER and LEON LAPIDUS

Princeton University, Princeton, New Jersey

Residence-time studies are reported for water trickling down through a 4-in. column packed with spheres. The transient response of the column to pulse- and step-function inputs in tracer concentration applied to the water stream was determined for both porous and nonporous packing. Significant radial variations in the distribution of residence times and the volumetric rate of flow were observed. The contribution to the response curves of diffusion into the porous packing and flow in the interparticle voids can be separated. The diffusion rates may then be characterized in terms of an effective pore diffusivity for the packing.

The present paper extends the data of a previous publication (*6*) dealing with the residence-time behavior of a nonreactive liquid trickling through a packed bed. The experimental procedure involves the predetermined addition of a tracer stream to the entering liquid and the subsequent time monitoring of the tracer composition in the bed effluent. Step and pulse additions of a variety of different tracers were used with water flowing through a 4-in. diameter bed packed with porous and nonporous packing.

A plot of effluent tracer concentration vs time of operation, referred to as a *time-of-contact* or *residence-time curve,* can be used to interpret a number of factors associated with the flow of liquid through the packed bed. In particular the shape of the effluent curve quantitatively defines the average distribution of liquid velocities within the bed, that is the approach to plug flow. Such data are of practical importance in determining the extent of a chemical reaction carried out under these hydrodynamic conditions. Further, the area under such a residence-time curve may be used to calculate the holdup of the flowing stream.

While a number of very definite results were concluded from the previous work, there were further points which could only be estimated because of the lack of appropriate or sufficient data. In particular it was shown that the fluid flow achieved a close approximation to plug flow. However the residence-time experiment only yields information on the average flow profile of fluid through the bed, and it is quite conceivable that there are appreciable radial variations which are not detected by this technique. Residence-time data are herein presented for discrete cylindrical sections of the packed bed which may then be compared with the overall result.

W. E. Schiesser is at Lehigh University, Bethlehem, Pennsylvania.

When the bed contains highly porous packing, the residence-time curve becomes a coupled function of the hydrodynamic flow of fluid through the bed and pore structure or diffusional properties of the packing. This results from the ability of the tracer to both move down the bed within the flowing stream and to diffuse into or out of the pore structure of the packing. A tentative conclusion reached from the previous data was that the coupled effects could be separated by a proper manipulation of the residence-time curve. In this way the effective pore diffusivity of the tracer could be estimated and the pore structure of the packing characterized. Completely independent data from a single agitated vessel as well as further residence-time data are herein presented to validate this conclusion.

Of paramount importance in the previous work was the observation that step and pulse forcing of the tracer inputs led to completely different residence-time curves when porous packing was used. This seems to imply that whereas the hydrodynamic and diffusional characteristics of the bed are linear when separated from each other, a coupling of the two processes produces a nonlinearity. It is very difficult however to conceive of a significant nonlinearity in this system with the components used. In the present paper an attempt is made to reconcile these seemingly contradictory points.

EXPERIMENTAL EQUIPMENT

A schematic diagram of the equipment is given in Figure 1. A 4-in. I.D. glass pipe, 48 in. in length, was used as the column in all of the experimental work. A liquid collector used for the determination of radial flow profiles consisted of seven concentric brass cylinders dimensioned so as to partition the cross section at the base of the column into seven equal circular areas. The cylinders were machined to $\pm$ 0.001 in. and had a wall thickness of 0.035 in. which was taken into account in the dimensioning for equal areas. The outermost cylinder fitted against the inside wall of the column to insure that the collector was centered at the base of the column. The top end of each of the cylinders was beveled to a sharp edge in order to partition the liquid at precise radial positions. Packing support rings were placed between the cylinders where needed to prevent particles of packing from dropping down into the collector.

Sampling of the effluent stream as a function of time was accomplished by means of one of two sampling wheels; the first held 4-in. test tubes for the simultaneous sampling of each of the seven streams flowing from the individual sections of the liquid collector. Successive rows of seven test tubes could be rotated under the sampling taps of the collector every 2 sec. (Figure 1). The second wheel, which held 125-ml. flasks, was used to sample the total effluent stream formed by merging the individual streams from the collector; a minimum sampling time of 1 sec. could be achieved.

Water was introduced onto the top of the packing from a flat perforated-plate distributor which gave a uniform flow rate per unit cross-sectional area except at the wall of the column. Eighteen 0.053-in. holes were drilled into the bottom plate of the distributor at carefully selected positions to achieve this uniformity of flow which is demonstrated by the radial flow profiles plotted in Figure 2. The percentage deviation of the flow rate in a given section of the collector from the average flow rate per section corresponding to a uniform profile is plotted against the number of the section for liquid rates of 9.28, 6.42, and 3.64 gal./min.-sq.ft. The two sets of profiles were obtained by operating the distributor at a position ½ inch above the collector, first with the ½-in. space empty, and then with a uniform layer of ¼-in. spheres on the top of the collector. The flow rate was essentially zero at the wall of the column because the outside diameter of the distributor was ⅛ of an inch less than the inside diameter of the column. Rubber spacers, 1/16 of an inch thick, were used to center the dis-

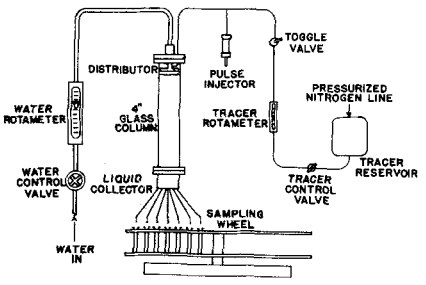

Fig. 1. Schematic diagram of experimental equipment.

tributor within the column during the experimental runs.

A step input of the tracer to the column was produced by the instantaneous opening and closing of a toggle valve on the tracer line. The pulse input to the column was produced by means of a piston type of injector made of brass; 9 cc. of concentrated tracer solution could be injected into the water entering the distributor in approximately ½ sec. with this device.

Water, which was the only liquid used in the experimental work, was taken directly from the laboratory lines for use in the column. Tracer solution was stored in a stainless steel reservoir which was pressurized with nitrogen to insure a steady flow rate. The dimensions of the materials used as packing in the column are given in Table 1.

EXPERIMENTAL PROCEDURE

Step- and Pulse-Function Responses

Reproducible transient response data were obtained by packing the column in the following manner. A single uniform layer of spheres was placed on the top of the liquid collector. The column was then filled with water and the packing slowly dumped into the desired height (36 in. unless otherwise specified). The taps on the collector were opened slightly so that water drained from the bottom of the column as the packing was added. Make-up water was continuously supplied at the top in order to maintain a constant water level within the column. The reproducibility of the transient response data was excellent when the column was repacked successively.

For the runs involving step forcing the column was operated at constant conditions for a minimum of 15 min. prior to the step input. For certain of these runs with porous packing and a low flow rate the preliminary period of operation was as high as 60 min. In all cases the initial operating time was substantially greater than the total transient response time of the column so that steady state conditions were assured at the instant the step input was applied. The tracer flow rate was 3% or less of the water rate in all of the runs.

For the runs involving pulse forcing the column was flushed with water for a minimum of 15 min. to insure that the packing was free of tracer prior to the injection of the pulse. The concentration and volume of the tracer solution injected into the column were noted for each run for subsequent use in the material-balance calculations.

The samples of the effluent stream were analyzed by one of two methods depending on the tracer used.

Sodium Chloride. The concentration of sodium chloride was determined by electrical conductivity to an accuracy of ± 1% over a concentration range of 0.940 to 0.00125 moles/liter. A conductivity probe was used for the analysis which could be inserted directly into the 4-in. test tubes used in the sampling wheel. The electrical resistance of the solutions was measured with a conductivity bridge. Precise temperature control was assured during the calibration of the probe and in the subsequent analysis of the effluent samples by immersing all of the solution in a constant-temperature bath maintained at 20.2° ± 0.02°C.

Each time effluent samples were analyzed the calibration of the analytical equipment was checked with standard resistances and standard hydrogen chloride solution. These maintained the analytical accuracy to within ± 1% or better.

Methyl Orange. The concentration of methyl orange was determined by colorimetry over a range of 0.00992 to 0.0000956 g./liter. An electrophotometer was used for the analysis. Of the four possible filters that could be used with this instrument, the blue filter (425-mμ. wave length) gave a maximum absorption with methyl orange.

Flow Profiles

The general shape of the flow profiles obtained with the liquid collector could be reproduced each time the column was repacked in the manner previously described. All of the flow profiles were obtained in the following manner. The flow rate from each of the seven sections of the collector was measured after the column was in operation at constant conditions for 15 min. The water was then turned off and the column allowed to drain for 5 min. Another set of flow rates was obtained at the end of a second 15-min. period of operation. The two sets of flow rates were then averaged for the final result.

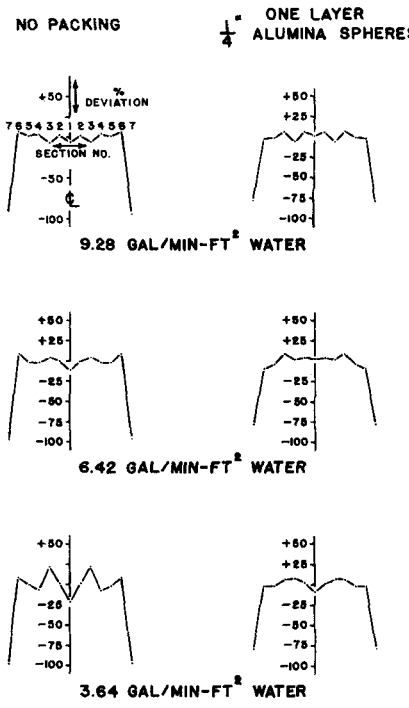

Fig. 2. Input flow profiles from the liquid distributor.

Effective Pore Diffusivities Measured in an Agitated Vessel

A number of experiments were performed in which the leaching of tracer from porous spheres suspended in the liquid of an agitated vessel was monitored. The porous spheres used in the agitated vessel were first weighed, then soaked in concentrated tracer solution for several days to insure complete saturation. The number of spheres used in an individual run varied from 100 for the

Table 1. Specifications of the Packing Materials

Manufacturer	Manufacturer's specification	Material	Nominal diameter, (in.)	Actual diameter (in.)
Scientific glass		glass	½	0.500
Norton	SA5203	alumina (porous)	½	0.490
Norton	SA5203	alumina (porous)	¼	0.257
Norton	LP	alumina (nonporous)	¼	0.234
Linde	4.A	molecular sieve	¼	0.208*

Porosity of the norton alumina spheres

Norton designation of composition	Nominal diameter	% porosity by water saturation	% porosity specified by Norton
SA5203	¼	45.0	45
SA5203	½	44.5	45

* The molecular sieve pellets were oblong in shape and varied considerably in size; this figure is the average of 200 measurements of the longest and shortest dimensions of 100 pellets sampled at random.

½-in. porous Norton spheres to 1,800 for the ¼-in. molecular sieves.

The agitated vessel, a 4,000-ml. beaker stirred by a flat-bladed impeller, contained 2,000 ml. of distilled water at the beginning of each run. The porous spheres, just before they were dumped into the beaker, were washed with four 500-ml. portions of distilled water to remove all of the tracer from the external surfaces. The length of the runs varied from 60 to 144 min. depending on the size and internal pore diameter of the spheres.

The maximum reduction in the volume of the solution in the beaker due to sampling was 7.7%. The reduction in the weight of the spheres due to attrition, determined by drying and weighing the spheres at the end of each run, was 9.1% and 5.5% for the ½- and ¼-in. Norton spheres, respectively, and 4.0% for the ¼-in. molecular sieves.

The effect of the solids attrition on the analytical determination of tracer concentration was determined by making duplicate runs with spheres that were initially soaked with distilled water. Electrical conductivity measurements made on the resulting samples indicated that the Norton spheres and molecular sieves are fabricated from materials which are highly insoluble in water; the resistance of these samples was not appreciably below that for the distilled water. The attrition did produce a turbidity in the samples which affected the colorimetric determination for methyl orange. This turbidity could be removed however by filtration with fine filter paper to the extent that the samples from the blank run gave 0% absorption on the colorimeter. All of the samples for the actual run with methyl orange were therefore filtered with the same filter paper before the colorimetric analysis, and it was assumed that any turbidity resulting from the solids attrition was completely removed.

Porosity of the Packing

The porosity of the ¼- and ½-in. Norton spheres was determined by measuring the difference in weight of the spheres when dry and when saturated with water. The measurements were repeated several times on each of three samples of ten spheres to check the reproducibility of the method. The final average results are tabulated in Table 1.

The porosity of the ¼-in. molecular sieves was not determined by the water-saturation method because of the irregularities in size and shape of the individual particles.

RESULTS AND DISCUSSION

Axial Hydrodynamic Conditions in the Trickle Bed

The approach to plug flow in any type of a tubular reactor is an important consideration in estimating the ultimate conversion level which can be achieved, since any dilution of the reactants by the products due to axial mixing will generally result in a reduced yield. The axial mixing in the liquid is a result of nonuniformities in flow velocity and holdup of the liquid in stagnant pools formed at the contact points of the packing. This axial mixing can be quantitatively evaluated from the response of the bed to a step- or pulse-function input if nonporous packing is used; the response is determined solely by the flow through the bed and mass transfer occurring in the interstices of the bed.

Table 2. Liquid Holdup in Beds of Various Heights: ¼-in. Nonporous Alumina Spheres

Bed height, (in.)	1 Uncorrected holdups, cu. ft. liquid/ cu. ft. bed	2 Holdups corrected for the external equipment, cu. ft.liquid/cu. ft. bed
36	0.162	0.162 − 0.065/3 = 0.140
24	0.175	0.175 − 0.065/2 = 0.143
12	0.204	0.204 − 0.065/1 = 0.139
0	0.065*	

* cu. ft. liquid/ cu. ft. bed.

The step response of the column when packed with ¼-in. nonporous alumina spheres is shown in Figure 3 for packing heights of 12, 24, and 36 in. These curves indicate the development of the front between pure and tracered water as the front moves down through the packed bed. These data may be replotted in terms of a dimensionless time t/θ_m with θ_m calculated from the material-balance equations below. Simpson's rule was used for numerical integration of the area under the step response curve:

$$H = \frac{V}{L}\int_0^\infty \frac{C}{C_o}\,dt = \frac{V}{L}\,\theta_m \qquad (1)$$

In particular a plot of ln C/C_o vs. t/θ_m for any experimental run yields a straight line. For the present data the slope of all of the straight lines is bounded between a value of −3.5 and −3.9. A value of −4.0 was reported by Lapidus for his experiments, and thus one may conclude that the main hydrodynamic effects are essentially the same for both setups.

In any tracer experiment of this type it is inevitable that the tracered stream must flow through a certain portion of the equipment which is outside the system of interest, the packed bed in this case. Ideally this external equipment should have no effect on the form of the tracer input function so that any distortion of the input which is observed in the effluent stream is caused only by the system under study. The curve in Figure 3 for zero packing height indicates that the effect of the holdup in the distributor and liquid collector was essentially that of a pure time delay of 3.1 sec., since the experimental step-input curve has nearly a vertical slope (time zero corresponds to the instant the tracer cut-off valve was closed). The ideal condition of negligible end effects was therefore closely approximated. However in order to obtain a liquid holdup which was independent of bed height it was necessary to take into account this time delay resulting from the external equipment. In column 1 of Table 2, the holdups for 12, 24, and 36-in. bed heights calculated by a numerical integration of the step response curves in Figure 3, are listed along with the holdup for the equipment calculated from the curve for zero packing. The true holdups in column 2 of Table 2, obtained by correcting for the equipment holdup, are independent of bed height. These values are larger than those reported by Lapidus, even though the residence-time curves exhibit approximately the same slope. As will be seen this is consistent with the higher liquid-solid contacting efficiencies found in the present investigation.

As previously mentioned the residence-time curves can be used to calculate the total holdup of liquid within the column [Equation (1) for a step input in tracer]. This total holdup is made up of the sum of the operating and static holdups as defined by Jesser

Table 3. Radial Flow Profiles for ¼-and ½-in. Nonporous Spheres in a 4-in. Column

Packing size, (in.)	Section number	1 ctr. line	2	3	4	5	6	7 wall
		Packing height—36 in. Flow rate—9.28 gal./min.—sq. ft.						
¼	Flow rate (cc./min.)	398	363	266	271	407	242	1018
	Percent of total flow = 42.5% from sections 6 and 7					Percent of total flow = 34.3% from section 7		
½	Flow rate (cc./min.)	375	208	298	198	297	614	994
	Percent of total flow = 54.2% from sections 6 and 7					Percent of total flow = 33.3% from section 7		

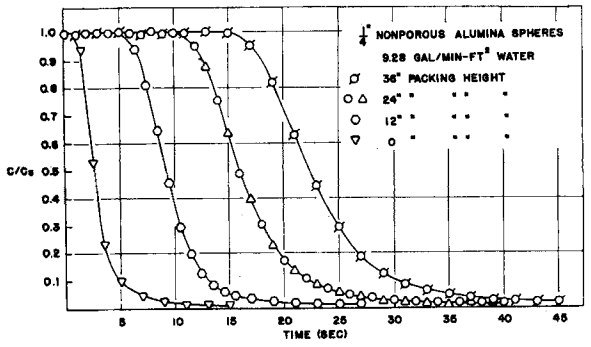

Fig. 3. Step response of the column for different packing heights.

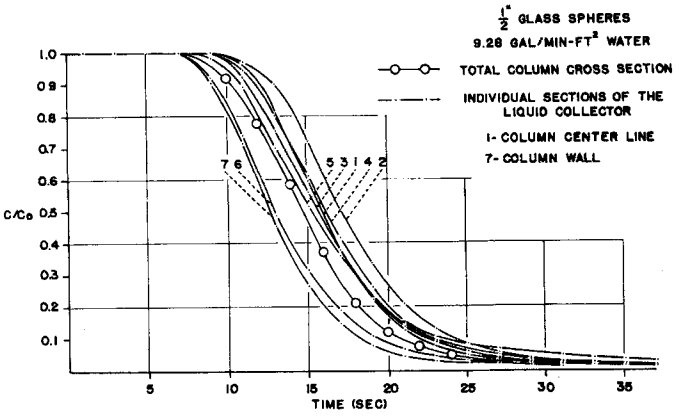

Fig. 4. Radial variation in the step response, $D_t/D_p = 8$.

and Elgin (5) and Shulman and coworkers (12). The operating holdup is that portion of the total holdup that moves quickly through the column, whereas the static holdup is the quantity of liquid held in stagnant pools at the contact points of the packing. The data of Shulman have indicated that the static holdup for a given packing is a constant independent of the liquid flow rate.

By use of the residence-time curves obtained in the present investigation for ½-in. glass spheres and the operating holdup reported by Jesser and Elgin the static holdup can be calculated. For data at five different flow rates the static holdup was calculated at 0.029 ± 0.002, thus substantiating the consistency of this factor.

Radial Hydrodynamic Conditions in the Trickle Bed

The close approach to plug flow indicated by the step-response curves for nonporous packing could be achieved even with substantial channeling within the packed bed or a disproportionate flow of the liquid down the walls of the column. Previous investigators who have used sectioned collectors for measuring the liquid flow rate at various points at the base of a packed bed have obtained conflicting results. Baker, Chilton, and Vernon (1) concluded on the basis of an experimental study made with a liquid collector consisting of a series of four concentric cylinders that wall effects are negligible for tube diameter to particle diameter ratios (D_t/D_p) greater than 10. This conclusion, which is probably the most commonly quoted design criterion for specifying the size of packing to be used in a column, was tested in the present study. The development of the radial flow profiles within the bed could be accurately determined since a well-defined input was used. The flow rate from each of the seven sections of the collector is given in Table 3 for a flow rate of 9.28 gal./min.-sq. ft. and for ½-in. glass spheres and ¼-in. alumina spheres (D_t/D_p ratios of 8 and 16 respectively). The conclusion of Baker et al. concerning a critical D_t/D_p ratio of approximately 10 was not confirmed since a heavy flow of water down the wall of the column was observed for a D_t/D_p ratio of 16. This result is not surprising in view of the significant increase in the void fraction at the column wall reported by Schwartz and Smith (11) for $D_t/D_p = 16$ and by Roblee, Baird, and Tierney (7) for $D_t/D_p = 13.6$. An improvement in the profile did result however from increasing the D_t/D_p ratio from 8 to 16. (The percentage of total flow from the two sections adjacent to the column wall was 54.2% for the ½-in. spheres and 42.5% for the ¼-in. spheres; 28.6% would correspond to a uniform profile.)

A significant difference was observed in the radial distribution of residence times for the ¼- and ½-in. spheres. The step-response curves for the individual sections of the liquid collector were spread out in time for the ½-in. spheres as shown in Figure 4, with the break occurring earliest in the two curves for the section closest to the wall. The maximum mean residence time was 18.0 sec. (section 2) and the minimum 13.4 sec. (section 7) or a difference of 29.3%. Thus the single experimental curve obtained for the total column cross section does not give an accurate indication of the true distribution in residence times of the tracer molecules passing through the bed. The greater uniformity in the density of the packing for the ¼-in. spheres due to a higher D_t/D_p ratio results in a more uniform response over the column cross section. These data are not shown, but the maximum mean residence time was 24.6 sec. (section 2) and the minimum 22.7 sec. (section 7) or a difference of 8.0%.

Of further interest is the fact that the individual residence-time curves for both size packings were parallel to each other. Thus there seems to be little radial mixing between streams flowing at different radial positions within the bed.

Table 4. Variation of the Liquid-Solid Contacting Efficiency with Flow Rate for ¼-in. Porous Alumina Spheres

Flow rate, min.-sq. ft.	Internal plus external holdup	External holdup	Internal holdup	Contacting efficiency, (%)
9.28	0.355	0.140	0.215	78.8
7.75	0.345	0.125	0.220	80.6
6.43	0.329	0.114	0.215	78.8
5.10	0.320	0.107	0.213	78.1
3.64	0.305	0.091	0.214	78.5

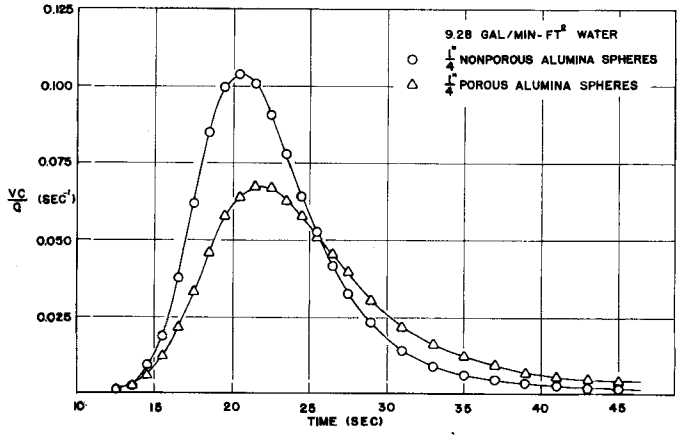

Fig. 5. Comparison of the pulse response for porous and nonporous packing.

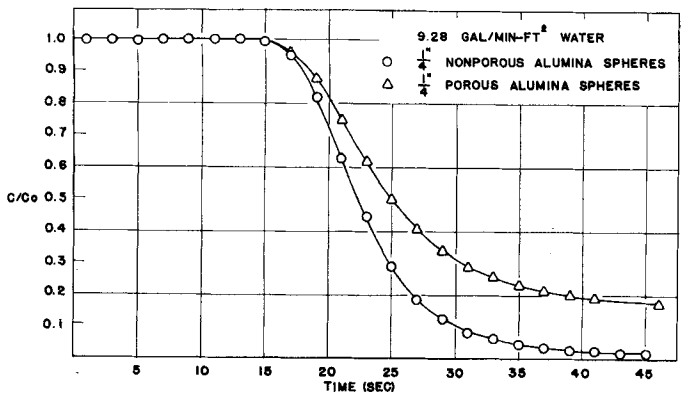

Fig. 6. Comparison of the step response for porous and nonporous packing.

Liquid-Solid Contacting Efficiencies with Porous Packing

If a step- or pulse-function input is applied to a fluid stream entering a column containing porous packing, the resulting response in the effluent stream will be determined by the flow of fluid in the external voids of the packing plus diffusion into and out of the pores of the packing. The contribution of pore diffusion to the transient response of the column can be determined by comparison of response curves for porous and nonporous packing obtained under identical operating conditions; in Figures 5 and 6 the pulse- and step-function response curves for a 36-in. bed of ¼-in. porous and nonporous alumina spheres are plotted for a liquid flow rate of 9.28 gal./min.-sq. ft. The quantity or holdup of liquid in the internal pores, as determined by the difference in areas under the step response curves, is 0.215 cu. ft. liquid/cu. ft. bed. The internal holdup for the limiting case when all of the pores are filled with liquid can be readily calculated by means of the equation

$$h_m = (1 - \epsilon)\,\gamma \qquad (2)$$

From Table 1 $\gamma = 0.450$ for ¼-in. porous alumina spheres. ϵ was determined for the nonporous spheres by water displacement to be 0.393; h_m is therefore equal to 0.273, and the percentage of the pores filled with liquid is 0.215/0.273 x 100 = 78.7%. This figure, which is the percentage of the packing that is effectively contacted by the flowing water stream, is above the maximum value of 54% reported by Lapidus. There are two possible reasons for this difference. Because of the differences in the packings the pore structure open for diffusion could also be quite different. The fraction of the pores contributing to the transient response would not be identical for the two packings thereby leading to different contacting values. The greater efficiency in the present case may also be due to the uniform flow from the distributor; if this is so, a strong point has been made in favor of careful distributor design. If this difference is due to the packings themselves, then these results indicate a greater accessibility of the present pores than those in the packing used by Lapidus.

The variation in liquid-solid contacting efficiency with flow rate was determined by a numerical integration of a series of step-response curves for ¼-in. nonporous and porous alumina spheres, the results are tabulated in Table 4. The contacting efficiency is essentially independent of the flow rate for the range of flow rates covered.

If the packed bed operates as a linear system; that is it is describable by a system of linear differential equations, the use of either pulse- or step-inputs in tracer should yield, after a simple transformation, identical residence-time curves. The holdup to a step is given by Equation (1) and that for a pulse by

$$H = \frac{V}{L}\int_0^\infty \frac{C}{C_o}\,dt = \frac{V}{L}\int_0^\infty \frac{V'}{Q}\int_0^t C_p\,dt\,dt \qquad (3)$$

Integration of the pulse response yields a curve identical in shape to the step response, whereas differentiation of the step response yields a curve comparable to the pulse response. Since numerical integration is a simpler and more accurate process than differentiation, a comparison is best made by converting the pulse responses to the form of the step. Figure 7 shows such a comparison for the case of nonporous packing for two different flow rates. The response curves are essentially identical, and thus the conclusion of Lapidus that the flow in a bed of nonporous spheres is a linear process is clearly confirmed.

In all of the pulse runs reported a material balance check was made between the quantity of tracer injected into the column and the quantity which appeared in the effluent stream. The mathematical statement of this balance is

$$\frac{V}{Q}\int_0^\infty C_p\,dt = 1.0 \qquad (4)$$

The value of this integral for the two response curves in Figure 7 is 1.005 and 0.986. The material balance for all of the pulse runs was 98% or better.

The data with porous packing lead to completely different results. When the hydrodynamic flow and the porous diffusion are coupled, the pulse-response curves are different from the step response. Such a difference implies that a nonlinear phenomenon may exist in the process. Since the data do not show a linear effect when porous packing is used, it is necessary to inquire into the reason for this. There are two possible causes for a nonlinear effect: adsorption of the tracer on a packing material in terms of a nonlinear isotherm and mass transfer into the porous packing. Both possibilities were investigated in the manner to be outlined. A preliminary test was per-

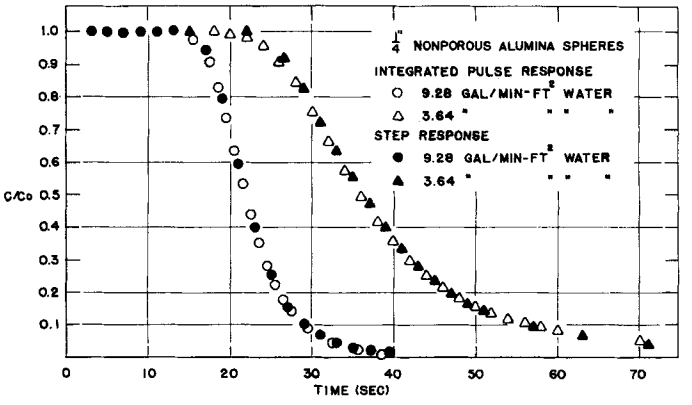

Fig. 7. Comparison of the step and integrated pulse response for nonporous packing.

formed to detect any adsorption of the tracer (sodium chloride) onto the surfaces of the porous packing; 500 dry ¼-in. porous alumina spheres were placed in a flask and covered with 0.2015 molar sodium chloride solution. The spheres were allowed to soak for several days, and at the end of this time the salt solution was found to still be 0.2015 molar. Any adsorption of the sodium chloride by the spheres would have reduced the concentration. Consequently adsorption is ruled out as a possible complicating factor in the comparison of the step and pulse responses to follow. Data presented in the next section indicate that this test was quite sensitive in the detection of adsorption effects or other combinations of packings and tracers.

This leaves mass transfer as a possible cause of a nonlinear effect. To test this point a series of runs was made with step- and pulse-function inputs applied to a 36-in. bed of ¼-in. porous alumina spheres. In order to determine any effect of concentration level on the diffusional mass transfer occurring within the porous packing, the intensity of the step- and pulse-function inputs was varied by changing the concentration and flow rate of the tracer solution entering the column. The direction of the step-function input was also reversed for several runs, that is a step up in tracer concentration or a step down.

The data for all of the runs with ¼-in. porous spheres are plotted in Figure 8 along with data for the ¼-in. nonporous spheres. The legend for Figure 8 indicates the type of input function, step and pulse; the intensity of the input, step—the value of C_o in moles sodium chloride/liter and pulse —the concentration of the tracer solution injected in moles sodium chloride/liter; the direction of the step input, designated as ⌐ and ⌙ for saturation and elution respectively; the value of the integral I:

$$I = \frac{V}{Q}\int_0^\infty C\,dt$$

$$= \frac{\text{moles of tracer in the effluent}}{\text{moles of tracer injected in the pulse}}$$

A perfect material balance for a pulse run corresponds to $I = 1$. The water rate for all of the runs was 9.28 gal./min.-sq. ft.

The step and integrated pulse responses for the porous packing are in good agreement over a relative concentration range of 1.0 to 0.1 corresponding to a time interval of 0 to 45 sec. (Figure 8); the response does not depend on the type or intensity of the input function. If however the data for the porous spheres are replotted with an extended time scale (Figure 9). significant differences can be observed between the response curves for the three input functions. These differences are more clearly indicated in Figure 10, where a single response curve for each of the three inputs has been plotted on semilogarithmic coordinates along with a single curve from Figure 8 for the nonporous packing. The holdup data in Table 5 provide a quantitative comparison of the difference in the transient response for the three input functions.

Table 5. Effective Internal Holdups for ¼-In. Porous Alumina Spheres Determined for Various Input Functions

Input function	External plus effective internal holdup, (Figure 9)	External holdup	Effective internal holdup	Apparent percentage of internal voids filled with liquid
Pulse	0.216	0.140	0.076	27.8
Saturation step	0.266	0.140	0.126	46.2
Elution step	0.355	0.140	0.215	78.8

On the basis of these results it must be concluded that there are no nonlinearities associated with adsorption or concentration effects. Since there is no question of the validity of the curves in Figures 8 to 10 (the curves being reproducible and the material balances checking out), it is necessary to look in a different direction for an explanation of the difference in the residence-time curves. A qualitative explanation may be suggested by the following. For the elution step inputs the flowing solution and the internal voids of the porous packing are initially filled with tracered liquid. When the input is stepped down in tracer concentration, the first result is to sweep tracer out of the flowing stream within the intervoids of the bed. This requires only a short period of time and leaves a situation very favorable to mass transfer of tracer out of the packing and into the flowing stream. Since this transfer process is relatively slow, the diffusion continues for a long time period and leads to an extended tail on the response curve. The holdup determined from the resultant residence-time curve is thus the sum of the external and the internal packing holdups. For the saturation step the last bit of tracer to diffuse into the packing cannot be detected because it is masked by the relatively large quantity of tracer in the liquid flowing through the interparticle voids. At the other extreme of a short width pulse input the pulse moves through the bed so rapidly that it is impossible for a significant portion of the tracer to diffuse from the flowing stream into the porous packing. In effect the pulse inputs are applied to a system involving only one time constant, the hydrodynamic flow time. The step inputs, by contrast, are applied to a system of coupled time constants involving hydrodynamic and diffusion times.

If such an explanation is correct, the pulse residence-time curves should approximate the curves for nonporous packing but with a slightly higher holdup due to the small amount of diffusion into the packing. From Figure 10 it can be seen that this is true. Further, the tailing on the elution-step curves should be characterized by a tracer diffusivity equivalent to pore diffusion within the packing. In a later section of this paper this hypotheses is shown to also be correct. As a final point if the width of the pulse is gradually increased, or for a constant width the flow rate is decreased, it would be expected that the resultant holdups would approach those for the elution-step inputs. A number of experimental runs were made in an effort to establish this trend. Whereas the step input yields a holdup of 0.215 irrespective of the flow rate, the pulse input yields a holdup of 0.076 at 9.28 gal./min.-sq. ft. and 0.142 at 6.42 gal./min.-sq. ft. These results show the expected trend.

The qualitative explanation presented for the difference in residence-time curves thus seems to agree with the available data. All efforts to construct a mathematical model, based on linear analysis, which fulfills these conditions have however proven fruitless.

Diffusional Mass Transfer Rates Within the Porous Packing as Determined from Transient Response Data

It was previously concluded that the low internal holdup from the pulse response corresponds to a partial penetration of the tracer into the porous packing. The elution-step input however resulted from diffusion of tracer initially distributed uniformly throughout the porous spheres. The elution-step response should therefore provide a true indication of the rate of diffusion within the porous packing. Two methods are presented for evaluating effective diffusivities from elution-step response data.

Rosen (*8, 9*) has formulated a mathematical model representing the mass transport processes which are in opera-

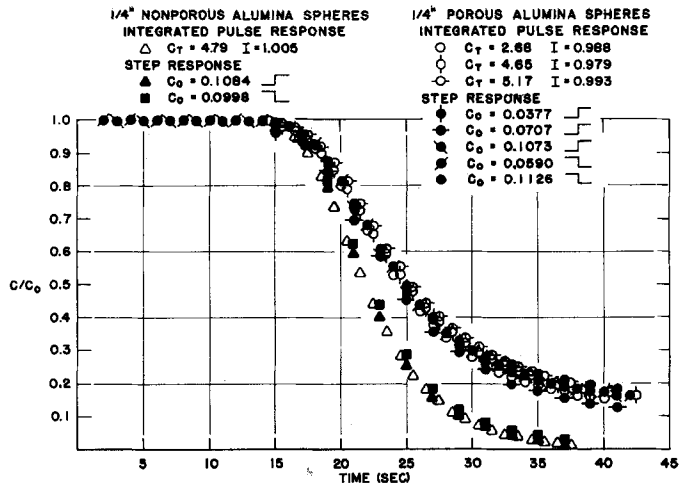

Fig. 8. Comparison of the step and integrated pulse response for porous packing, short time scale.

tion when a single fluid phase flows through an idealized bed of porous spheres. The basic assumptions inherent in the model are all of the mass transfer processes are linear, a uniform velocity profile, and no axial mixing. The transient step response of the model bed was determined by solving appropriate differential material-balance equations subject to a step-function input. The solution for the case of negligible resistance to mass transfer between the fluid and the porous spheres is

$$\frac{C(x,t)}{C_o} = \frac{\exp\left[Y\lambda_o^2/2 - X(A+1)\right]}{\left\{2\pi\left[1+\frac{X}{4}(A+B-2AB)\right]\right\}^{1/2}} \qquad (5)$$

where λ_o is the root of

$$Y\lambda^2 - XA\lambda - B\lambda - 2 = 0$$

Equation (5) is applicable to the case of two-phase flow through a bed of porous spheres if the quantities z/v and m are modified:

single-phase	two-phase
$z/v = \theta_m$	$zH_t/V = \theta_m$
$m = \epsilon/1-\epsilon$	$m = H_t/1-\epsilon$

Equation (5) is plotted in Figure 11 in terms of the dimensionless variable Y/X with X as a parameter. The experimental data for a 36-in. bed of ¼-in. porous alumina spheres are also plotted in Figure 11 for a flow rate of 9.28 gal/min.-sq.ft. The slopes of the experimental and theoretical curves can not be matched exactly, but an approximate value of X can be estimated; an effective pore diffusivity can then be calculated, since all of the other quantities in X are known. For $X = 0.03$, $D = 2.9 \times 10^{-5}$ sq. cm./sec. for sodium chloride diffusing in water.

A semiempirical method for estimating effective pore diffusivities may be developed from the Einstein equation:

$$D = \overline{X^2}/2t \qquad (6)$$

D can be calculated if $\overline{X^2}$ and t are suitably chosen. It can be shown (*10*) that

$$\sqrt{\overline{X^2}_m} = r_o/4 \qquad (7)$$

where $\sqrt{\overline{X^2}_m}$ is the average root mean square displacement for the total sphere. The value of the diffusion time to be used is suggested by the semilogarithmic plot of the step-response data for ¼-in. porous and nonporous alumina spheres. Since all of the data were obtained under the same operating conditions, the break in the response curve for the porous spheres is due to the diffusional mass transfer within the intraparticle voids. Furthermore the slope of the lower curve must be a measure of the rate of diffusion within the internal voids. The reciprocal of the slope (189 sec.), which is a characteristic time constant for diffusion, can therefore be used in Equation (6) for calculation of the diffusivity:

$$D = \frac{X^2}{2t} = \frac{\left(\frac{1}{4}r_o\right)^2}{2t}$$

$$= \frac{\left(\frac{1}{4}\times\frac{0.257}{2}\times 2.54\right)^2}{2\times 189}$$

$$= 1.76\times 10^{-5} \text{ sq.cm./sec.}$$

which compares favorably with the value of 2.9×10^{-5} sq. cm./sec. determined from Rosen's theoretical curves.

For the case of data with ½-in. porous alumina spheres the reciprocal of the slope of the residence time curve is 750 sec. These data yield a diffusivity of 1.61×10^{-5} sq.cm./sec.

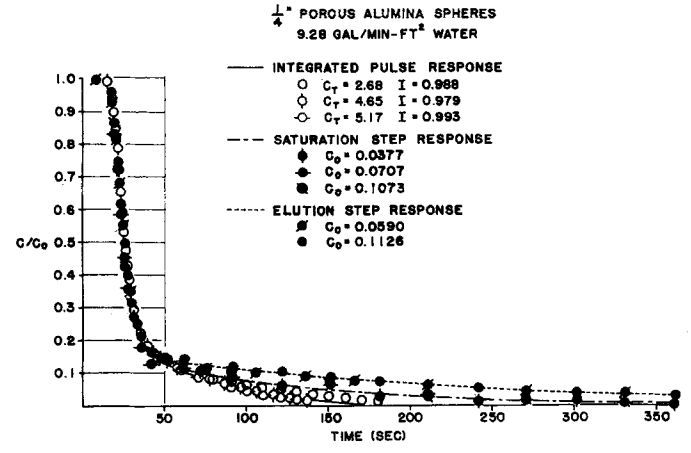

Fig. 9. Comparison of the step and integrated pulse responses for porous packing, long time scale.

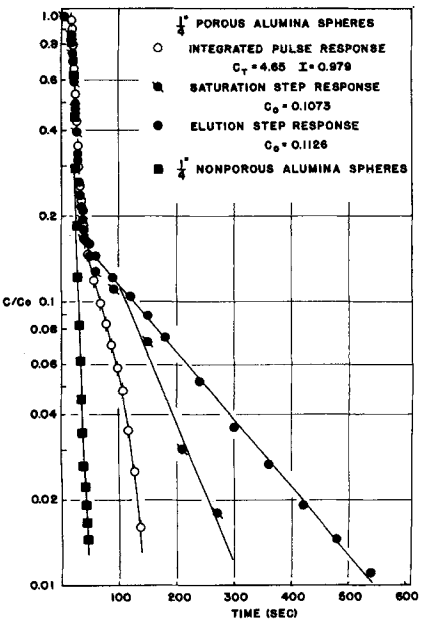

Fig. 10. Comparison of the step and integrated pulse responses for porous packing, semilogarithmic plot.

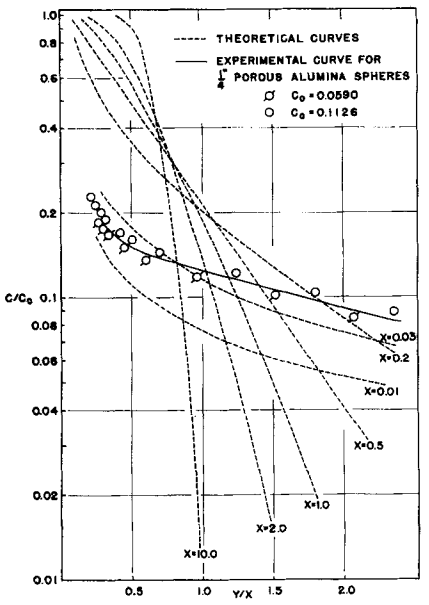

Fig. 11. Comparison of the experimental and theoretical step response curves for porous packing.

Since the terminal portion of the step response provides a direct indication of the rate of diffusion within the porous packing, it should also directly indicate the rate of diffusion-controlled reaction. This point has been verified experimentally by Blue et al. (2) who found that the slope of the elution-step response curve of a fixed-bed reactor was equal to the apparent rate constant for two diffusion-controlled gas-phase reactions occurring in the reactor. Furthermore it was found that the rate constant and the slope of the step-response curve varied in exactly the same way with catalyst particle size. The present relationship between the reciprocal slope of the step response, the particle size, and the effective pore diffusivity therefore provides a convenient means for estimating the apparent rate of a diffusion-controlled reaction. Specifically the rate constant can be estimated simply from a knowledge of the catalyst particle size and the effective pore diffusivity for the catalyst. The productive capacity of a reactor can therefore be estimated from information which is readily available if the chemical reaction is controlled by the diffusion within the catalyst.

Diffusional Mass Transfer Rates Within The Porous Packing as Determined from an Agitated Vessel

The use of an agitated vessel for the evaluation of effective pore diffusivities insures that all resistances to mass transfer other than the internal pore diffusion are eliminated. This method therefore provides a reliable check of the diffusivities determined from the transient response of the column where several mass transfer processes are in operation simultaneously.

The solution to the diffusion equation for the case of a porous sphere initially saturated with tracer solution, placed in an agitated volume of liquid, initially free of tracer is (3)

$$\frac{C}{C_o} = 1 - 6a(a+1) \sum_{n=1}^{\infty} e^{-Da^2_n t} \frac{1}{a^2 r^2_o \alpha^2_n + 9(a+1)} \qquad (8)$$

where α_n, $n = 1, 2, 3, \ldots$, are roots of

$$\tan(r_o \alpha) = \frac{3 r_o \alpha}{3 a r^2_o \alpha^2}$$

Equation (8) is plotted in Figure 12 in terms of the dimensionless variable Dt/r^2_o for $a = \infty$. The experimental data for the ¼- and ½-in. porous alumina spheres are also included in Figure 12. Diffusivities of 1.43×10^{-5} and 1.70×10^{-5} sq.cm./sec. (sodium chloride in water) for the ¼- and ½-in. spheres respectively, determined from the best fit of the experimental data to the theoretical curve, are in good agreement with the diffusivities determined from the step-function response of the packed column.

The free diffusivity of sodium chloride in water reported (4) for 0.05 molar concentration at 18°C. is 1.26×10^{-5} sq.cm./sec. It is interesting to compare this value with those calculated for pore diffusion. In order to make this comparison it is necessary to convert the pore diffusivities from units of square centimeters solid per second to square centimeters liquid per second. This requires that the intraparticle void fraction and the contacting efficiency be used. For the ¼-in. porous alumina spheres $\gamma = 0.450$ and $\eta = 0.788$. The results are given in Table 6.

The diffusivities listed in columns 2 and 3 indicate that the porous structure of the alumina spheres had only a moderate effect on the diffusional mass transfer rate. As expected the free diffusivity is greater than the calculated pore diffusivities.

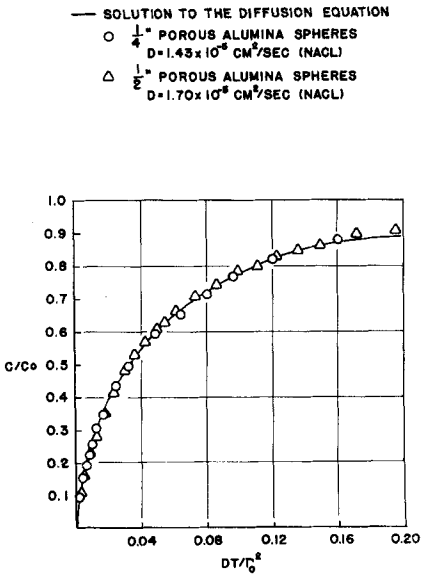

Fig. 12. Pore diffusivities measured in an agitated vessel, sodium chloride tracer.

Diffusional Mass Transfer Rates Within the Porous Packing: Effect of Tracer and Pore Diameter on the Diffusional Mass Transfer

The transient response of a bed of porous spheres for a given set of operating conditions will be determined by the type of tracer that is used. The effect of the tracer on the observed rate of diffusion within the porous alumina spheres was determined by methyl orange, an organic compound with a relatively high molecular weight of 327.3, as a second tracer for comparison with sodium chloride. The step-function response of the column when packed with ¼-in. porous alumina spheres was obtained for two tracer concentration levels (C_o) of 0.00917 and 0.01764 g./liter. The two response curves are not identical because of a slight adsorption of the methyl orange onto the surface of the alumina packing. The test previously

Table 6. Correction of Effective Pore Diffusivities for the Volume Occupied by the Solid

Method of evaluation	1 Pore diffusivity, (sq. cm. solid/sec.)	2 $\gamma \times$ Pore diffusivity, (sq. cm. liquid/sec.)	3 Free-liquid diffusivity, (sq. cm. liquid/sec.)
Rosen's theoretical curves	2.9×10^{-5}	1.0×10^{-5}*	1.26×10^{-5}
Semi-empirical method	1.76×10^{-5}	0.625×10^{-5}*	1.26×10^{-5}
Agitated vessel	1.43×10^{-5}	0.644×10^{-5}	1.26×10^{-5}

* The liquid-solid contacting efficiency was included.

Table 7. Variation of the Sodium Chloride Diffusivity with Pore Diameter

Packing material	Average pore diameter, (Å.)	Effective pore diffusivity
¼-in. alumina spheres	125,000 (*10*)	1.76×10^{-5}
⅛-in. cobalt molybdate-activated cracking catalyst	macro pore structure 2000 (*5*)	1.70×10^{-5} (reported by Lapidus)
	micro pore structure 100 to 200	
¼-in. molecular sieves	4	2.35×10^{-6}

described for the detection of adsorption effects gave a 2.7% decrease in the concentration of the methyl orange solution used to saturate a sample of the alumina spheres. The diffusivities estimated from the slopes of the curves are 1.34×10^{-5} and 1.41×10^{-5} sq. cm./sec. as compared with 0.835×10^{-5} sq. cm./sec. measured in the agitated vessel.

The effect of the pore diameter on the rate of diffusion was investigated with ¼-in. molecular sieves for comparison with the porous alumina spheres. The diffusivity (sodium chloride) estimated from the slope of the step-response curve is 2.35×10^{-6} sq. cm./sec. as compared with 2.55×10^{-6} sq. cm./sec. measured in the agitated vessel. This relatively low rate of diffusion for the molecular sieves is probably due to a Knudsen effect; the mean free path of the tracer ions is greater than the average pore diameter so that the ions collide with the pore walls rather than with the water molecules and with each other. Since the mean free path in the liquid state is of the order of molecular dimensions, a packing with a pore diameter greater than several molecular diameters should not exhibit Knudsen diffusion. The data in Table 7 substantiate this point. The microporous structure of the cobalt molybdate catalyst (pore diameter of 100 to 200 Å) did not exert a retarding effect on the diffusion.

Since the average diameter of the methyl orange molecule is considerably greater than 4 Å., the molecular sieves should give the same transient response as a nonporous packing if methyl orange is used as the tracer. Unfortunately an experimental verification was not possible because the methyl orange was strongly adsorbed onto the external surfaces of the molecular sieves. The adsorption test gave a 90.7% reduction in the concentration of the methyl orange solution. A similar test for the sodium chloride gave no indication of adsorption by the molecular sieves.

CONCLUSIONS

The present residence-time data for a liquid trickling through a packed bed show that significant radial variations in flow rate exist for a particle-to-tube radius as large as 1:16. Methods are discussed for separating the hydrodynamic and diffusional contributions to the residence-time curves when porous packing is used. This allows a characterization of the pore structure of the packing by an effective diffusivity based upon relatively simple experimental tests.

ACKNOWLEDGMENT

This investigation was made possible through the financial support generously provided by the California Research Corporation and the Monsanto Chemical Company for which the authors are very grateful.

The authors would also like to thank Dr. C. A. Sleicher, Jr., of the Shell Development Company for detailed written communications on the material in this paper.

NOTATION

C = transient effluent tracer concentration at time t resulting from a step input; for agitated vessel, concentration in vessel at time t

C_o = steady state influent and effluent tracer concentration for a step input; for agitated vessel, final concentration in solution

C_p = transient effluent tracer concentration at time t resulting from a pulse input [Equation (3)]

D_c/D_p = tube to particle diameter ratio

D = effective pore diffusivity

H = total liquid holdup [Equation (1)]

h_t = total external holdup, determined for nonporous packing

I = numerical value of material balance integral [Equation (4)]

L = bed length

N = number of spheres used in agitated vessel

Q = moles tracer injected in pulse input

V = volumetric flow rate of liquid (cu.ft. liquid/sq.ft. bed-sec.) = volume of liquid in agitated vessel in Equation (8)

V' = volumetric rate, (cu.ft./sec.)

$\bar{X}^2$ = mean square displacement of a tracer molecule from its initial position in a porous sphere

a = ratio of liquid volume in agitated vessel to volume of liquid in sphere $= 3V/4\pi r_o^3\gamma$

h_m = maximum internal pore holdup

m = interparticle void volume per unit volume of solid particles

r_o = radius of porous spheres

t = time of operation

x = linear flow velocity of fluid stream

z = distance down the bed measured from the top

θ_m = mean residence time of tracer molecules in the bed

γ = internal (intraparticle) void fraction of packing

ϵ = external (interparticle) void fraction of packing

η = contacting efficiency

In Equation 5

A = $\lambda_o \coth \lambda_o$

B = $(\lambda_o \operatorname{csch} \lambda_o)^2$

X = $3D\ \gamma z/mvr_o^2$, bed-length parameter (dimensionless)

Y = $2D(t - z/v)r_o^2$, contact-time parameter (dimensionless)

LITERATURE CITED

1. Baker, Theodore, T. H. Chilton, and H. C. Vernon, *Trans. Am. Inst. Chem. Engrs.*, **31**, 296 (1934-35).
2. Blue, R. W., V. C. F. Holm, R. B. Reiger, E. Fast, and L. F. Heckelsberg, *Ind. Eng. Chem.*, **44**, 2710 (1952).
3. Carslaw, H. S., and J. C. Jaeger, "Conduction of Heat in Solids," 2 ed., p. 240, Oxford at the Clarendon Press, England (1959).
4. "International Critical Tables," Vol. 5, p. 67, McGraw-Hill, New York (1933).
5. Jesser, B. W., and J. C. Elgin, *Trans. Am. Inst. Chem. Engrs.*, **39**, 277 (1943).
6. Lapidus, Leon, *Ind. Eng. Chem.*, **49**, 1000 (1957).
7. Roblee, L. H. S., R. M. Baird, and J. W. Tierney, *A.I.Ch.E. Journal*, **4**, 460 (1958).
8. Rosen, J. B., *J. Chem. Phys.*, **20**, 387 (1952).
9. ——, *Ind. Eng. Chem.*, **46**, 1590 (1954).
10. Schiesser, W. E., Ph.D. dissertation, Princeton Univ., Princeton, New Jersey (1959).
11. Schwartz, C. E., and J. M. Smith, *Ind. Eng. Chem.*, **45**, 1209 (1953).
12. Schulman, H. L., C. F. Ullrich, and N. Wells, *A.I.Ch.E. Journal*, **1**, 247 (1955).

Manuscript received February 24, 1960; revision received June 20, 1960; paper accepted June 24, 1960. Paper presented at A.I.Ch.E. Mexico City meeting.